Geophysical Research Letters

RESEARCH LETTER
10.1029/2019GL081960

Special Section:
Bridging Weather and Climate: Subseasonal-to-Seasonal (S2S) Prediction

A Modeling Strategy for the Investigation of the Effect of Mesoscale SST Variability on Atmospheric Dynamics

Yinglai Jia[1], Ping Chang[2,3], Istvan Szunyogh[3], R. Saravanan[3], and Julio T. Bacmeister[4]

[1]Physical Oceanography Laboratory, Ocean University of China, Qingdao, China, [2]Department of Oceanography, Texas A&M University, College Station, TX, USA, [3]Department of Atmospheric Sciences, Texas A&M University, College Station, TX, USA, [4]Climate and Global Dynamics Division, National Center for Atmospheric Research, Boulder, CO, USA

Key Points:
- An atmospheric GCM coupled to a slab ocean model can be used to study the effect of mesoscale SST variability on atmospheric dynamics
- SST mesoscale variability has a significant effect on components of the atmospheric circulation that play roles in S2S predictability

Correspondence to:
I. Szunyogh,
szunyogh@tamu.edu

Citation:
Jia, Y., Chang, P., Szunyogh, I., Ramalingam, S., & Bacmeister, J. T. (2019). A modeling strategy for the investigation of the effect of mesoscale SST variability on atmospheric dynamics. *Geophysical Research Letters*, *46*, 3982–3989. https://doi.org/10.1029/2019GL081960

Received 30 JAN 2019
Accepted 24 MAR 2019
Accepted article online 28 MAR 2019
Published online 1 APR 2019

Abstract An efficient modeling strategy is proposed for the investigation of the effect of the sea surface temperature (SST) mesoscale variability on atmospheric dynamics. Two ensembles of numerical simulations are generated with a high-resolution atmospheric global circulation model coupled to a slab ocean model. The two ensembles differ only in the treatment of the SST data used for the specification of the SST initial conditions and the estimation of the oceanic heat transport: one of the ensembles is generated by retaining, while the other by filtering, the mesoscale SST variability. The effect of mesoscale SST variability is assessed by comparing the two ensembles. The strategy is illustrated by simulation experiments with the Community Earth System Model, with a focus on the processes of the NH midlatitudes. The results suggest that ocean mesoscale variability has a significant effect on the jet streams, large-scale flow, and midlatitude storm tracks.

1. Introduction

Improving operational subseasonal-to-seasonal (S2S) predictions has been a top priority of weather forecasting research (e.g., Roberston & Vitart, 2018; White et al., 2017). Accounting for midlatitude mesoscale ocean-atmosphere interactions in the forecast models is considered a potential way to make progress toward this goal (Saravanan & Chang, 2018). We propose to employ a high-resolution atmospheric general circulation model that is thermodynamically coupled to a slab ocean model to test this hypothesis. The motivation to consider a slab rather than a full ocean model is threefold, as for a slab ocean model (1) the systematic sea surface temperature (SST) errors (biases) are easier to manage (Zuidema, 2016), (2) the computational expense is significantly lower, and (3) oceanic initial conditions are necessary only for the SST. In this pilot study, we present simulation results with the proposed coupled system to show that it is able to maintain midlatitude mesoscale SST variability and that variability has significant effects on atmospheric processes that play a role in S2S predictability.

There exists ample evidence that atmospheric variability at timescales longer than 5–7 days can be affected by oceanic feedback. For instance, Mosedale et al. (2006) investigated the variability of the North Atlantic Oscillation (NAO), which has an *e*-folding time of about 10 days (Feldstein, 2000), by coupled climate model simulations and found that the oceanic feedback led to a 10–30% increase of the seasonal variance of the NAO. This increase of the variability was consistent with the results of an earlier simple model study (Barsugli & Battisti, 1998) that showed that coupling a stochastic atmospheric model to a slab ocean with finite heat capacity increased atmospheric variability. It has also been shown that the sharp SST gradients along the oceanic fronts in the midlatitudes play a major role in anchoring the midlatitude atmospheric storm tracks through their effect on baroclinicity in the lower troposphere (Nakamura et al., 2004). In addition, it has been found that SST anomalies associated with ocean mesoscale variability can lead to a strong atmospheric response (Chelton & Xi, 2010; Chelton et al., 2004; Small et al., 2008; Xie, 2004). In particular, Ma et al. (2015, 2017) showed that mesoscale SST variability along the Kuroshio Extension region can exert a significant downstream influence on winter rainfall variability along the U.S. Northern Pacific coast, while Foussard et al. (2019) obtained similar results by idealized channel model experiments.

Our proposed modeling strategy builds on that of Ma et al. (2015, 2017). They carried out two sets of atmospheric ensemble simulations with the limited area Weather Research and Forecasting (WRF) model at a horizontal resolution of 27 km. While one set of simulations was forced by 0.09° resolution SST analyses, which resolved mesoscale SST variability, the other set of simulations was carried out by

suppressing the mesoscale SST variability by spatial filtering. We make two changes to this experiment design. First, we employ a state-of-the-art global atmospheric model, the Community Earth System Model (CESM) of the National Center for Atmospheric Research (NCAR), which provides a realistic representation of the large-scale atmospheric dynamics that plays a central role in S2S predictability. Second, rather than prescribing the SST, we allow for two-way thermodynamical interactions between the ocean and atmosphere.

The structure of the paper is as follows. Section 2 explains the proposed modeling strategy and describes its implementation on the CESM. Section 3 presents simulation results for this implementation, and section 4 offers our conclusions.

2. Modeling Strategy

2.1. Slab Ocean Model

A slab ocean model has a single prognostic state variable: the temperature of the ocean mixed layer, the SST. The related prognostic equation is the first law of thermodynamics for the ocean mixed layer, which is

$$\frac{\partial T_{\text{mixed}}}{\partial t}(\mathbf{r},t) = \frac{1}{\rho c_0 h_{\text{mixed}}(\mathbf{r})}\left[Q_{\text{atm}}(\mathbf{r},t) - Q_{\text{ocn}}(\mathbf{r},t)\right], \tag{1}$$

where $\mathbf{r}$ is the two-dimensional vector of horizontal location, t is time, $T_{\text{mixed}}(\mathbf{r},t)$ is the SST, ρ is the density of the ocean water, c_0 is the specific heat of the ocean water, $h_{\text{mixed}}(\mathbf{r})$ is the depth of the ocean mixed layer, $Q_{\text{atm}}(\mathbf{r},t)$ is the net heat transfer from the atmosphere to the mixed layer, and $Q_{\text{ocn}}(\mathbf{r},t)$ is the net (horizontal and vertical) heat transfer to other parts of the ocean. Describing the spatiotemporal evolution of the SST by equation (1) requires the knowledge of both $Q_{\text{atm}}(\mathbf{r},t)$ and $Q_{\text{ocn}}(\mathbf{r},t)$. $Q_{\text{atm}}(\mathbf{r},t)$ can be computed online in a coupled simulation as

$$Q_{\text{atm}}(\mathbf{r},t) = Q_{\text{sol}}(\mathbf{r},t) - Q_{\text{long}}(\mathbf{r},t) - Q_{\text{sen}} - Q_{\text{latent}}(\mathbf{r},t), \tag{2}$$

where Q_{sol} is the net radiative heating of the ocean mixed layer by solar radiation, Q_{long} is the net long-wave radiative cooling of the ocean mixed layer, Q_{sen} is the net sensible heat flux from the ocean to the atmosphere, and Q_{latent} is the net latent heat flux from the ocean to the atmosphere. $Q_{\text{ocn}}(\mathbf{r},t)$, however, has to be prescribed, that is, precomputed off-line.

2.2. The Computation of $Q_{\text{ocn}}(\mathbf{r},t)$

In the proposed strategy, an ensemble of uncoupled atmospheric model simulations is carried out to obtain an ensemble of $Q_{\text{atm}}(\mathbf{r},t)$ for a set of different atmospheric initial conditions but for the same single time series of SST analyses. The ensemble mean of $Q_{\text{atm}}(\mathbf{r},t)$ provides an estimate of $Q_{\text{atm}}(\mathbf{r},t)$ that is independent of the atmospheric initial condition. The prescribed $Q_{\text{ocn}}(\mathbf{r},t)$ is computed by solving equation (1) for $Q_{\text{ocn}}(\mathbf{r},t)$, making use of the aforementioned estimate of $Q_{\text{atm}}(\mathbf{r},t)$ and an approximate value of $\partial T_{mixed}/\partial t(\mathbf{r},t)$ that can also be computed from the time series of SST analyses. In practice, in addition to accounting for the heat transfer in the ocean, the $Q_{\text{ocn}}(\mathbf{r},t)$ computed by the process described here also corrects for the biases in $Q_{\text{atm}}(\mathbf{r},t)$. (The online calculated value of $Q_{\text{atm}}(\mathbf{r},t)$ in the coupled calculations will typically be different from the one used in this step.)

2.3. Generation of the Control and Filtered Ensemble

The calculation of $Q_{\text{ocn}}(\mathbf{r},t)$ is done twice: for a time series of high-resolution SST analyses that resolve mesoscale variability, and for a spatially filtered version of the same data that no longer resolve mesoscale variability. The resulting pair of $Q_{\text{ocn}}(\mathbf{r},t)$ is then used to generate a pair of ensemble simulations. The two ensembles use the same ensemble of (different) atmospheric initial conditions. The effect of mesoscale SST feedback to the atmosphere can be assessed by comparing ensemble statistics for the two ensembles.

2.4. CESM Implementation

We generate the control and filtered ensemble for the month of December 2007. We choose this particular period because it corresponds to an unstable epoch of the Kuroshio Extension, in which Kuroshio eddies are very active and mesoscale SST anomalies are strong, but the El Niño–Southern Oscillation and the Pacific Decadal Oscillation are nearly neutral. We note that the simulations of Ma et al. (2015) were also carried out for this period.

We use daily, 0.25° × 0.25° resolution, 0000 UTC NOAA Optimum Interpolation Sea Surface Temperature and ICE (OISSTV2) analyses as SST data. The SST field of the filtered simulations is obtained by applying a 5° × 5° boxcar filter to the data. We carry out experiments with the beta_02 version of CESM1.3, which includes the latest version of the atmospheric model CAM5 (CAM5.3.06) and a slab ocean model option, at horizontal resolution 0.23° × 0.23° with 30 vertical model levels.

In equation 1, $\rho = 1,026\ \mathrm{kg/m^3}$, $c_0 = 3930\ \mathrm{J{\cdot}kg^{-1}{\cdot}K^{-1}}$, and $h_{\mathrm{mixed}}(\mathbf{r})$ is determined from the Levitus (1982) Climatological Atlas of the World Ocean. (For reference, h_{mix} is about 50 m in the Kuroshio Extension region and over 300 m in the North Atlantic region.) For the estimation of $Q_{\mathrm{ocn}}(\mathbf{r}, t)$, the approximate value of $\partial T_{\mathrm{mixed}}/\partial t$ is calculated from the SST analyses, first for 0000 UTC of each day and then to each time step of the simulations by linear interpolation. We start the estimation of $Q_{\mathrm{atm}}(\mathbf{r}, t)$ by an integration of the atmospheric model from 0000 UTC 15 November, 2007 to 2400 UTC 30 December, 2007, using a climatological mean state as atmospheric initial condition. We consider the first 15 days of model integration a "spin-up" period and obtain a 10-member ensemble of atmospheric initial conditions for 0000 UTC 1 December 2007 by changing the date associated with the model states at every third day of the remaining 30 days of the simulation to 0000 UTC 1 December 2007. These initial conditions are used for the generation of a 10-member ensemble of 30-day atmospheric simulations (ending at 2400 UTC 30 December, 2007). We compute $Q_{\mathrm{atm}}(\mathbf{r}, t)$ for each ensemble member by equation (2), and use the ensemble mean as the estimate of $Q_{\mathrm{atm}}(\mathbf{r}, t)$ for the computation of $Q_{\mathrm{ocn}}(\mathbf{r}, t)$.

Both the control and filtered ensemble have 30 members: each member is a coupled simulation from 0000 UTC 1 December 2007 to 2400 UTC 30 December 2007. The different atmospheric initial conditions of the two ensembles are obtained by changing the dates associated with the 0000 UTC atmospheric states from the last 30 days of the 45-day atmospheric simulation that provided the initial conditions for the estimation of $Q_{\mathrm{atm}}(\mathbf{r}, t)$ to 0000 UTC 1 December 2007. The common SST initial condition of the control ensemble is defined by the 0.23° × 0.23° resolution SST analysis for 0000 UTC 1 December 2007, while the common SST initial condition of the filtered ensemble is defined by the filtered version of the same analysis. Because CESM includes an elastic viscous plastic dynamics model of sea ice, we also have to provide an initial condition for the ice concentration at 0000 UTC 1 December 2007. We obtain this initial condition by an integration of the CESM with the slab ocean model, using $Q_{\mathrm{con}}(\mathbf{r}, t)$ for the filtered SST and the default ice initial condition of the model until the ice concentration resembles the observed ice concentration for December 2017.

3. Results

3.1. SST Bias

We measure the SST bias at a particular geographical location by the time-mean difference between the ensemble mean of the simulated SST and the analyzed SST. We compute the time-mean for only week 3 and 4 of the simulations to reduce the effect of transient model behavior on the calculated means. We find that the magnitude of the SST bias is within 2 °C at all locations for both ensembles (Figures 1a and 1b). In addition, the main patterns of SST biases are similar for the two ensembles. The differences between the biases of the two simulations are equal to the time-mean differences of the two ensemble means (Figure 1c). As expected based on equation (1), these differences have the same spatial structure as the time-mean difference field of $-Q_{\mathrm{ocn}}$ (not shown) for the two ensembles. In the midlatitudes, the two difference fields either resemble mesoscale ocean eddies (e.g., in the Kuroshio extension region) indicate differences in the gradients associated with oceanic fronts (e.g., Gulf Stream) or reflect larger scale differences of Q_{ocn} between the two experiments (e.g., north of Hawaii).

3.2. SST Ensemble Spread

Because all members of the control or filtered ensemble use the same SST initial condition and prescribed oceanic heat transport, SST differences between the ensemble members develop in response to the differences in $Q_{\mathrm{atm}}(\mathbf{r}, t)$, or more generally, the atmospheric state. These differences grow rapidly with time in both ensembles (Figures 1d and 1f), which indicates a strong thermodynamical response of the slab ocean to the atmospheric state. Interestingly, the growth of the ensemble spread is somewhat faster for the filtered ensemble, which suggests that the atmospherically forced SST variability is stronger when no mesoscale ocean features are present. In addition, except for the first few days, the analyzed SST stays within one standard deviation from the ensemble mean for both ensembles, which indicates that the ensemble members describe plausible evolutions of the SST.

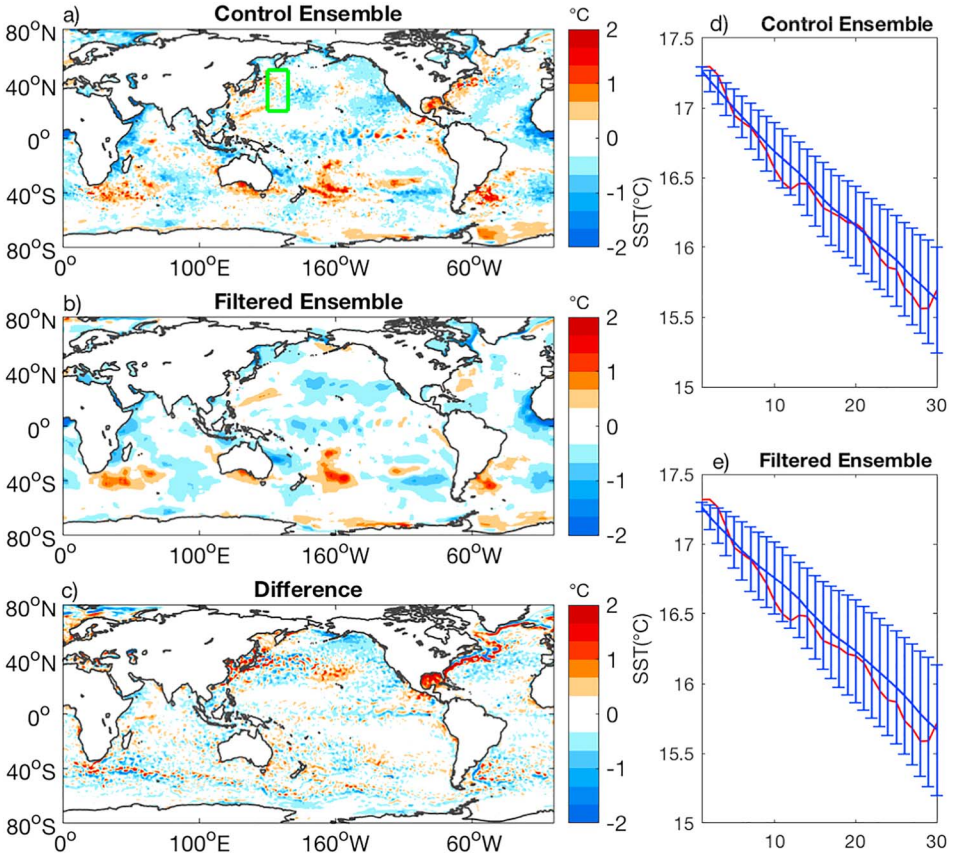

Figure 1. Diagnostics of the simulated SST. Color shades show the fields of the SST bias for the (a) control and (b) filtered ensemble, and (c) the differences between panels a and b (°C). The blue lines show the ensemble mean and the bars the ensemble spread of the areal mean SST in the Kuroshio Extension for the (d) control and (e) filtered ensemble. The areal mean is calculated for the region (green rectangle in a) defined by latitudes 20–50°N and longitudes 150–165°E. The red lines show the areal mean SST for the (d) unfiltered and (e) filtered SST analysis in the same region. SST = sea surface temperature.

3.3. Biases of the Atmospheric State

Similar to our approach for the SST, we measure biases of the simulated atmospheric state by the time-mean difference between the ensemble means and the analyses of the state variables. The results for the zonal component of the wind at 300 hPa (Figure 2, contour lines) show that the locations of the jet streams are generally well captured by the two simulations (Figures 2b and 2c), although the Pacific jet does not extend as far to the east in the two simulations as in the analyses (Figure 2a) and the core of the Atlantic jet stream is also somewhat stronger in the two simulations. The results for the mean-sea-level pressure (Figure 2, color shades) suggest that the major large-scale pressure systems are also well simulated except for an underestimated Aleutian Low and an overly zonal NAO phase.

3.4. Atmospheric Effects of the Ocean Mesoscale Feedback

We assess the effects of ocean mesoscale variability on the atmospheric circulation by examining differences between time and ensemble average diagnostics of selected atmospheric state variables for the two ensembles for week 3 and 4. We test the statistical significance of the differences between the averages (estimates of the means) by applying a two-sample *t* test to the pair of samples composed of the pair of 0000 UTC ensemble mean values of the state variable for each day of weeks 3 and 4. We account for the temporal correlations in the samples by assuming that they are the results of a first-order autoregressive process (e.g., Wilks, 1982, Example 5.2). The locations where the differences are significant at the 95% level are marked by gray dots in the maps that show the differences. We also performed a Wilcoxon rank sum test, but the results are not shown, because they were in good agreement with those for the *t* test.

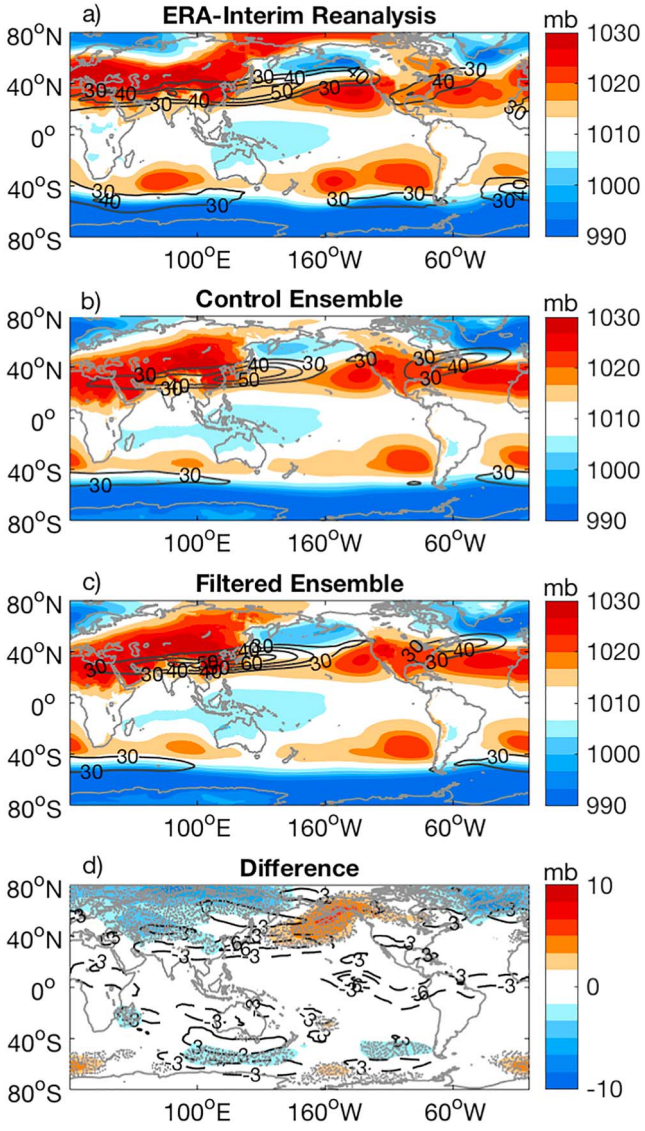

Figure 2. The effect of ocean mesoscale variability on the jet streams and large-scale pressure systems. Contour lines show the time- and ensemble mean of the zonal wind component at 300 hPa (m/s) and color shades the time- and ensemble mean of the mean-sea-level pressure. The two fields are shown for (a) the ERA-Interim Reanalysis (Dee et al., 2011), and the mean of the (b) control and (c) filtered ensemble. Also shown (d) are the differences between panels b and c (positive values indicate higher values for the control ensemble).

The results show that ocean mesoscale variability has a major effect on the simulated atmospheric circulation (Figure 2d). In particular, it weakens the jet stream of the North Pacific by about 10%, while leaving the jet stream of the Atlantic largely unaffected (contour lines). In addition, it makes the atmospheric flow north of 40°N more zonal by making the Aleutian low shallower (color shades), reducing the mean-sea-level pressure elsewhere (color shades), and increasing the zonal wind speed at some locations at around 60°N. The largest local difference in the Aleutian low is almost 10 mb.

Because a weaker jet stream produces a weaker tropospheric vertical wind shear, an application of the classical theory of baroclinic instability (Charney, 1947; Eady, 1949) would suggest that ocean mesoscale feedback should reduce the intensity of the midlatitude storm tracks. Contrary to this expectation, the results indicate that the feedback increases the eddy kinetic energy associated with the 300-hPa meridional component of the wind (Figure 3), which is a measure of the intensity of the storm tracks. A possible explanation for this paradoxical result lies in the effect of moisture on baroclinic instability: diabatic heating associated with the

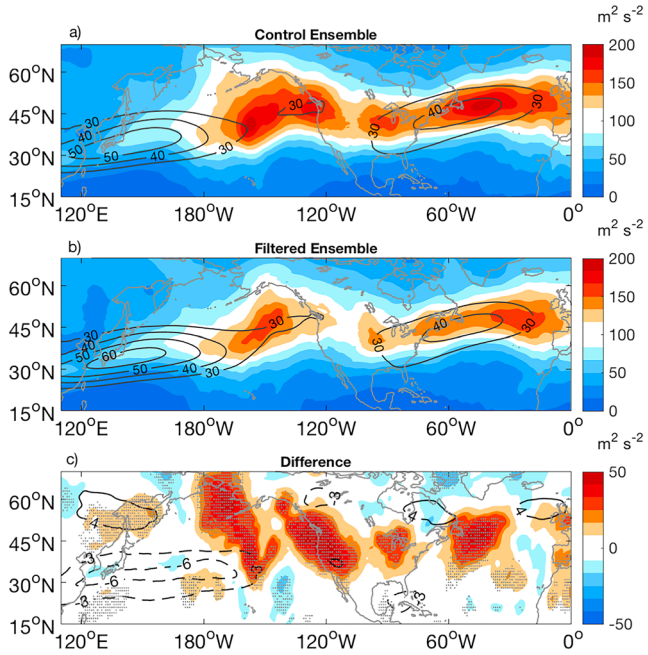

Figure 3. The effect of ocean mesoscale variability on the intensity of the midlatitude storm tracks in the NH. Contour lines show the time- and ensemble mean of the 300-hPa zonal wind (m/s) and color shades the time- and ensemble mean of the eddy kinetic energy $\frac{1}{2}v'^2(\mathbf{r},t)$ for the meridional component $v(\mathbf{r},t)$ of the wind at 300 hPa. The eddy component of the meridional wind $v'(\mathbf{r},t)$ is defined by the difference between the daily 0000 UTC values of $v(\mathbf{r},t)$ and their temporal mean for weeks 3 and 4. The fields are shown for the (a) control and (b) filtered ensemble. Also shown (c) are the differences between the fields of panels a and b (positive values indicate higher values for the control ensemble).

presence of moisture can increase the intensity of baroclinic growth (e.g., Ahmadi-Givi et al., 2004; Mak, 1994; Snyder & Lindzen, 2008; Willison et al., 2013). Most importantly for our study, Ma et al. (2015, 2017) showed that the presence of Kuroshio mesoscale eddies can lead to an increase of the moisture content of the atmospheric boundary layer, which in turn enhances cyclonegenesis via moist baroclinic instability.

We test our conjecture about the role of atmospheric moisture by examining the effect of ocean mesoscale feedback on the moist atmospheric processes in our experiments (Figure 4). In the Kuroshio extension region, the mesoscale eddies increase the total precipitable water content of the atmosphere (Figure 4a), which is the result of a significant increase of the specific humidity below 800 mb (Figure 4b). The latter diagnostics is for a zonal line segment along 38°N, which is marked by a green line in Figure 4a, where eddy-induced mesoscale SST variability is particularly high in both the simulations (Figure 4c, blue line) and the observation-based SST analyses (same panel, red line). (The good agreement between the blue and red line confirms that the slab ocean model simulates the SST variability with high fidelity.) Quantitatively, the increase of moisture in the control ensemble amounts to about 15% of the total precipitable water of the filtered ensemble. Our results show that ocean mesoscale variability affects the moisture content of the lower troposphere by enhancing the vertical moisture fluxes (Figure 4d) at all locations. Comparing Figures 4b and 4c, it is evident that the moisture fluxes are enhanced, because positive (negative) spatial SST anomalies always lead to positive (negative) spatial moisture anomalies and upward (downward) relative motions. Finally, we note that we have not found increased precipitation associated with the increased amount of total precipitable water in the Kuroshio region. This result suggests that other processes, such as atmospheric moisture transport, act as a local sink of the extra atmospheric moisture added in that region.

4. Conclusions

In this pilot study, we tested a modeling strategy to investigate the effect of ocean mesoscale variability on S2S predictability. We first demonstrated that it was feasible to design experiments in which the proposed

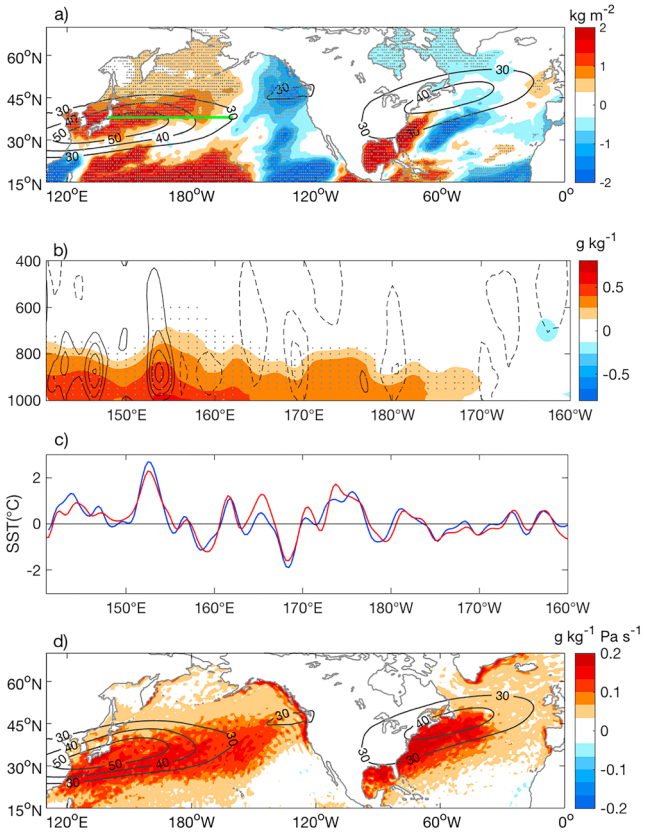

Figure 4. The effect of ocean mesoscale variability on the moist atmospheric processes in the North Pacific and Atlantic region. All panels show time-mean diagnostics. (a) Color shades show the differences between the control and filtered ensemble mean for the vertically integrated total precipitable water, while the contour lines indicate the location of the jet streams by showing the zonal wind speed (m/s) for the control ensemble at 300 hPa. (b) Color shades show the vertical profile of the differences between the ensemble means for the specific humidity along the zonal segment marked by a green line in panel (a), while contour lines show the related differences for the vertical wind speed (the contour interval is $2 \times 10^{-}2$ Pa/s and positive values indicate relative upward motion in the control ensemble). (c) To highlight the relationship between the diagnostic of panel (b) and the mesoscale SST anomalies along the line segment, the blue (red) line shows the difference between the mean SST of the two ensembles (the high-resolution and filtered analysis). (d) Color shades show the differences between the two ensembles for the vertical moisture flux at 850 hPa (positive values indicate higher values for the control ensemble), while the contour lines are the same as in panel (a). SST = sea surface temperature.

coupled system maintained a low SST bias and realistic mesoscale SST variability. We then found that ocean mesoscale variability had statistically significant effects on the North Pacific jet stream, the zonality of the atmospheric flow north of 40°N, and the intensity of the midlatitude storm tracks. While some of the specific effects are likely to be flow dependent, they are the type of effects that have potentially important influences on S2S predictability.

As the role of particular dynamical processes are concerned, we found in good agreement with Ma et al. (2015, 2017) and Foussard et al. (2019) that midlatitude ocean mesoscale eddies enhanced the moisture fluxes in the lower troposphere. A plausible explanation for the increased intensity of the midlatitude storm tracks in our experiments is that the enhanced moisture fluxes led to more intense baroclinic energy conversion in the entrance regions of the midlatitude storm tracks. We further speculate that the vertical atmospheric motions induced by ocean mesoscale variability may excite vertically propagating gravity waves that could lead to a gravity wave drag on the large-scale atmospheric flow. Such a drag could explain the weakening of the North Pacific jet observed in our experiments. Finally, we note that to the best of our knowledge, a parameterization for the enhanced moisture fluxes induced by unresolved ocean mesoscale variability is not included in the global circulation models, which may have a negative effect on the quality of lower resolution model simulations.

Acknowledgments
The critical comments of the two anonymous reviewer helped greatly improve the presentation of our results. This research has been conducted as part of the NOAA MAPP S2S Prediction Task Force and supported by NOAA grant NA16OAR4311082. Yinglai Jia was supported by National Key R&D Program of China (2017YFC1404101), and the Strategic Priority Research Program of the Chinese Academy of Sciences (Grant XDA11010203). The data used for the preparation of the figures are publicly available (https://doi.pangaea.de/10.1594/PANGAEA.897395).

References

Ahmadi-Givi, F., Craig, G. C., & Plant, R. S. (2004). The dynamics of a midlatitude cyclone with a very strong latent-heat release. *Quarterly Journal of the Royal Meteorological Society*, *130*, 295–323.

Barsugli, J. J., & Battisti, D. S. (1998). The basic effects of atmosphere-ocean thermal coupling on midlatitude variability. *Journal of the Atmospheric Sciences*, *55*, 477–493.

Charney, J. G. (1947). The dynamics of long waves in a baroclinic westerly current. *Journal of Meteorology*, *6*, 371–385.

Chelton, D. B., Schlax, M. G., Freilich, M. H., & Milliff, R. F. (2004). Satellite measurements reveal persistent small-scale features in ocean winds. *Science*, *303*, 978–983.

Chelton, D. B., & Xi, S. P. (2010). Coupled ocean-atmosphere interactions at oceanic mesoscales. *Oceanography*, *23*, 52–69.

Dee, D. P., Uppala, S. M., Simmons, A. J., Berrisford, P., Poli, P., Kobayashi, S., & Vitart, F. (2011). The ERA-Interim reanalysis: Configuration and performance of the data assimilation system. *Quarterly Journal of the Royal Meteorological Society*, *137*, 553–597.

Eady, E. T. (1949). Long waves and cyclone waves. *Tellus*, *1*, 33–52.

Feldstein, S. B. (2000). The timescale, power spectra, and climate noise properties of teleconnection pattern. *Journal of Climate*, *13*, 4430–4440.

Foussard, A., Lapeyre, G., & Plougonven, R. (2019). Storm track response to oceanic eddies in idealized atmospheric simulations. *Journal of Climate*, *32*, 444–463.

Levitus, S. (1982). Climatological Atlas of the world ocean (*NOAA Professional Paper 13*). Washington D. C.: U.S. Government Printing Office. 173 pp.

Ma, X., Chang, P., Saravanan, R., Montuoro, R. ., Hsieh, J.-S., Wu, D., et al. (2015). Distance influence of Kuroshio eddies on North Pacific weather patterns. *Scientific Report*, *5*, 17785.

Ma, X., Chang, P., Saravanan, R., Montuoro, R. ., Nakamura, D., Wu, D., et al. (2017). Importance of resolving Kuroshio front and eddy influence in simulating North Pacific storm tracks. *Journal of Climate*, *30*, 1861–1880.

Mak, M. (1994). Cyclogenesis in a conditionally unstable moist baroclinic atmosphere. *Tellus*, *46A*, 14–33.

Mosedale, T. J., Stephenson, D. B., Collins, M., & Mills, T. C. (2006). Granger causality of coupled climate process: Ocean feedback on the North Atlantic Oscillation. *Journal of Climate*, *19*, 1182–1194.

Nakamura, H., Sample, T., Tanimoto, Y., & Shimpo, A. (2004). Observed associations among storm tracks, jet streams and midlatitude oceanic fronts. In C. Wang, S. P. Xie, & J. A. Carton (Eds.), *Earth's climate: The ocean-atmosphere interaction* (pp. 329–345). Washington, DC: American Geophysical Union.

Roberston, A. W., & Vitart, F. (Eds.) (2018). *Sub-seasonal to seasonal prediction: The gap between weather and climate Forecasting* A. W. Roberston & F. Vitart (Eds.) (585 pp.). Amsterdam: Elsevier.

Saravanan, R., & Chang, P. (2018). Midlatitude mesoscale ocean-atmosphere interaction and its relevance to S2S prediction. *In Roberston and Vitart*, *2018*, 183–200.

Small, R. J., deSzoeke, S. P., Xie, S. P., O'Neill, L., Seo, H., Song, Q., et al. (2008). Air-sea interaction over ocean fronts and eddies. *Dynamics of Atmospheres and Oceans*, *45*, 274–319.

Snyder, C., & Lindzen, R. S. (2008). Quasi-geostrophic wave-CISK in an unbounded baroclinic shear. *Journal of the Atmospheric Sciences*, *48*, 76–86.

White, C. J., Carlsen, H., Robertson, A. W., Klein, R. J. T., Lazo, J. K., Kumar, A., et al. (2017). Potential applications of subseasonal-to-seasonal (S2S) predictions. *Meteorological Applications*, *24*, 315–325.

Wilks, D. S. (1982). *Statistical methods in the atmospheric sciences* (2nd ed., pp. 627). Amsterdam: Academic Press.

Willison, J., Robinson, W. A., & Lackman, G. M. (2013). The importance of resolving mesoscale latent heating in the North Atlantic storm track. *Journal of the Atmospheric Sciences*, *70*, 2234–2249.

Xie, S. P. (2004). Satellite observations of cool ocean-atmosphere interaction. *Bulletin of the American Meteorological Society*, *85*, 274–319.

Zuidema, P. (2016). Challenges and prospects for reducing coupled climate model SST biases in the eastern tropical Atlantic and Pacific Oceans: The U.S. CLIVAR Eastern Tropical oceans Synthesis Working Group. *Bulletin of the American Meteorological Society*, *97*, 2305–2327.